



Equipment-free and visual detection of multiple biomarkers via an aggregation induced emission luminogen-based paper biosensor

Haiyin Li, Haiyang Lin, Wenxin Lv, Panpan Gai, Feng Li^{*}

College of Chemistry and Pharmaceutical Sciences, Qingdao Agricultural University, Qingdao, 266109, PR China

ARTICLE INFO

Keywords:

Aggregation induced emission
Dopamine
Inner filter effect
Paper biosensor
Equipment-free
Visual detection

ABSTRACT

Early and accurate disease diagnosis is of great appeal for saving patients' life, but requires biomarkers to be sensitively detected with simplicity, convenience, and low cost. Exploring the development of a high-performance fluorescence biosensor for biomarkers solid, equipment-free and visual biosensing is highly urgent but faces enormous challenges. Herein, we proposed a brand-new fluorescence system by integrating a typical aggregation induced emission dye (TPE-BTD) with dopamine for multiple biomarkers sensitive detection based on target-induced catalyzing oxidation. The system comprising TPE-BTD and dopamine emits strong fluorescence; with horseradish peroxidase (HRP) or HRP-mimicking DNAzyme and H_2O_2 being added, significant oxidation on dopamine occurs to generate dopachrome, which actuated the inner filter effect (IFE) due to the overlap of its absorption curve and emission spectrum of TPE-BTD, subsequently decreasing fluorescence emission and displaying a rapid and sensitive response to H_2O_2 and G-quadruplex DNA. We further apply TPE-BTD/dopamine system in analysis of glucose and DNA adenine methylation methyltransferase (Dam MTase) based on target-initiated signal transduction. Finally, TPE-BTD was employed as emitters in fabrication of paper biosensors, which can achieve solid, equipment-free and visual detection of multiple biomarkers based on the high emission performance of TPE-BTD, opening up a new pathway to development of biosensors for practical application. We expect this sensing conception will be helpful in development of practical biosensors, and this sensor will find more applications in disease diagnosis.

1. Introduction

With the significant advancement of basic biomedical science, more and more information evidenced the pivotal role of biomarkers in effecting the early and accurate determination of various diseases due to their earlier appearance of change in expression level than organization or morphology (Broza et al., 2019; Das and Singal, 2004; Liu et al., 2014; Wu and Qu, 2015). Unfortunately, traditional approaches such as computed tomography, nuclear magnetic resonance imaging, and B-ultrasound cannot meet the requirement because of the low sensitivity, high cost, complex and professional procedures. Featured with simplicity, rapidity, and high sensitivity, fluorescence technique has become a popular paradigm for various diseases diagnosis compared with traditional and other modern techniques (Adhikary et al., 2010; Chang et al., 2019; Chinen et al., 2015; Feng et al., 2018b; Li et al., 2019; Tagit and Hildebrandt, 2017; Wang et al., 2015; Yang et al., 2019; Zang et al., 2019; Zhang et al. 2016, 2019). Nevertheless, some intrinsic matters remain to preclude their bright prospect in application of

clinical diagnosis and treatment. For example, current available methods primarily used conventional fluorescent dyes as emitters, which are limited by serious aggregation caused quenching (ACQ) and poor photobleaching resistance. Moreover, these dyes needed to be labeled with deoxyribo nucleic acid (DNA) or peptide or other biomolecules, the process of which is complicated and tedious. As such, fluorescence sensors currently remain two significant challenges: complex labeling procedure and lacking high emission-performance materials.

In the past decade, plenty of work has been done to explore high-performance fluorescence materials, such as carbon dot, quantum dot, metal cluster or complex (Ghosh et al., 2019; Huang et al., 2014; Lemon et al., 2015; Miao et al., 2018; Muthusankar et al., 2020; Shahrokhiana et al., 2018; Zhang et al., 2018). These materials have proven to be capable of enhancing the sensitivity to a certain level, but weak emission, high toxicity, and poor stability force us to rethink the simple yet ingenious strategy for high-performance materials fabrication. Aggregation induced emission luminogen (AIEgen) possesses the unique

^{*} Corresponding author.

E-mail address: lifeng@qau.edu.cn (F. Li).

<https://doi.org/10.1016/j.bios.2020.112336>

Received 28 April 2020; Accepted 27 May 2020

Available online 2 June 2020

0956-5663/© 2020 Elsevier B.V. All rights reserved.

characteristic of weak or non-emissive in dissolved state and high emission performance in aggregated state, with strong anti-fade and anti-photobleaching properties, and thus, is considered as an ideal candidate for high-performance biosensor (Ding et al., 2013; Feng et al., 2018a). It is expected that integration of AIEgen into a biosensor would realize the win-win of amplified detection and decreased incidence of misdiagnosis (Min et al., 2015; Niu et al., 2020). As such, substantial time and effort have been dedicated to developing AIEgen-based fluorescence sensors (Shi et al., 2017; Zhu et al., 2020). Among them, one effective approach is to label AIEgen with biomolecules. However, the label process is unfavorable due to the disadvantages mentioned above. Another strategy is to prepare positively charged AIEgens, which can electrostatically interact with negatively charged biomolecules without the need for labeling. Besides, Liu's group prepared a tyrosine-functionalized TPE-Tyl for label-free detection of H_2O_2 , glucose, and human carcinoembryonic antigen (Wang et al., 2014); our group developed a label-free fluorescence biosensor for microRNA assay based on a maleimide-functionalized AIE material (Li et al., 2018). Undoubtedly, application of AIEgens in fluorescence analysis enables simple, low-cost, and sensitive detection of biomarkers. Whereas, it is noted that these sensors obliged AIEgens to be modified with functional groups, and thus, suffered from high-price fabrication, tedious procedure, and strict reaction condition. More notably, most of previously reported AIEgens are applied as emitters in solution state, and these solution systems require expensive instruments and professional technicians to conduct fluorescence measurements, making detrimental to practical application outside the laboratory (Hu et al., 2014; Jia et al., 2019; Paroloa and Merkoçi, 2013).

Herein, in this study, we successfully prepared a typical AIE dye (TPE-BTD), and integrated it with dopamine to develop a high-performance biosensor for label-free and sensitive detection of multiple analytes in solution state and solid state based on target-initiated catalyzed oxidation. TPE-BTD, comprising tetraphenylethene and benzothiadiazole moieties, displayed bright emission at 550 nm with absolute quantum yield of 0.2311 and lifetime of 0.9608 ns. However, its emission can be quenched by dopachrome generating from the catalyzing oxidation of horseradish peroxidase (HRP) and H_2O_2 on dopamine based on inner filter effect (IFE) due to the overlap of emission spectrum of TPE-BTD and UV-vis curve of dopachrome, demonstrating highly sensitive response to H_2O_2 . Since hemin/G-quadruplex possesses high HRP-like activity, G-quadruplex DNA and H_2O_2 can generate through target-switched transduction reaction (Albada et al., 2016; Golub et al., 2011), TPE-BTD/dopamine system could be applicable for G-quadruplex DNA and other biomarkers biosensing. Further, TPE-BTD and dopamine were integrated into cellulose paper to fabricate paper biosensors for solid, equipment-free and visual detection of multiple biomarkers.

2. Experimental

2.1. Preparation of TPE-BTD

Vinyl-functionalized tetraphenylethene (TPE-V) (0.8953 g) and 4,7-dibromo-2,1,3-benzothiadiazole (BTD-2Br) (0.291 g) were dissolved in 50 mL of dimethylacetamide (DMAC). After that, anhydrous K_2CO_3 (0.4146 g) and tetrabutylammonium bromide (0.10 g) were added. The reaction solution was stirred in an N_2 environment for 30 min, followed by addition of catalytic amount $\text{Pd}(\text{OAc})_2$. The mixed solution was then permitted to react at 120 °C for 48 h to obtain an orange power with a yield of 41% through purification. ^1H NMR (500 MHz, CDCl_3) δ (ppm): 6.99 (d, 4H), 7.11 (m, 6H), 7.26 (m, 12H), 7.42 (t, 20H), 7.68 (d, 2H); ^{13}C NMR (125 MHz, CDCl_3) δ (ppm): 108.3, 126.3, 126.4, 127.2, 127.4, 128.0, 128.7, 134.4, 139.2, 140.0, 152.8; FT-IR (KBr) ν (cm^{-1}): 2812, 2721, 1704, 1595, 1485, 1437, 1027, 761, 701.

2.2. Fluorescence detection of target biomarkers in solution

For H_2O_2 assay, the procedure was described as follows. 80 μL of 10 mM phosphate buffer (PB) (pH 7.4) containing 0.125 mM dopamine (DA) and 0.125 mg/mL horseradish peroxidase (HRP), and 1.0 μL of TPE-BTD (0.50 mM) solution in dimethyl sulfoxide (DMSO) were mixed together. After that, 19 μL of H_2O_2 solution with different concentrations was added, and the resulting solution was allowed to react for 5 min at 37 °C before fluorescence measurement.

For the detection of glucose, a sensing solution was prepared by mixing 80 μL of 10 mM PB containing 0.125 mM dopamine, 0.125 mg/mL HRP and 1.25 $\mu\text{g/mL}$ glucose oxidase (GOx), and 1.0 μL of TPE-BTD solution (0.50 mM, DMSO). Subsequently, 19 μL of glucose solution with different amounts was dropped into the solution to incubate for 20 min at 37 °C before fluorescent measurements.

For the detection of G-quadruplex DNA, 80 μL of 10 mM PBS (50 mM NaCl, 50 mM MgCl_2 , 100 mM KCl, pH 7.4) containing 0.125 mM dopamine and 1.25 mM H_2O_2 , and 1.0 μL of DMSO solution containing 0.20 mM hemin and 0.50 mM TPE-BTD were mixed together. Then 19 μL of G-quadruplex DNA solution with different concentrations was added, and the mixture was allowed to react for 10 min at 37 °C before fluorescent measurements.

For the detection of DNA adenine methylation methyltransferase (Dam MTase), the recognition and cleavage reactions were in progress in a 20 μL of 10 mM PBS (50 mM NaCl, 10 mM MgCl_2 , pH 7.4) consisting of 1.0 μM ON1, 1.0 mM dithiothreitol (DTT), 80 μM S-adenosyl methionine (SAM), 80 U/mL DpnI, and target analyte with different levels for 2.0 h. Subsequently, 50 μL of 10 mM PBS containing 800 nM ON2, 0.1 U/mL klenow fragment (KF) polymerase, 0.6 U/mL Nb.BbvCI Nease, and 350 μM dNTPs was added into the above 20 μL of solution and the mixed solution was allowed to incubate for 1.5 h at 37 °C. Right after the two steps, the mixture was heated and maintained the temperature at 90 °C for 10 min to diminish the affect of thiol compounds on sensing results. Finally, 29 μL of PB containing 3.33 mM H_2O_2 and 0.345 mM dopamine, and 1 μL of DMSO solution containing 0.2 mM hemin and 0.5 mM TPE-BTD were successively dropped into the above mixed solution, and the resulting solution reacted for 10 min before fluorescence measurement.

2.3. Solid detection based on the TPE-BTD-based paper biosensor

3 μL of TPE-BTD solution (50 μM) and 3 μL of 10 mM PB containing 2.0 mM dopamine and 1 mg/mL HRP were successively dropped onto the surface of cellulose paper, and the fabricated paper biosensor was denoted as TDH-PS. Then 3 μL of H_2O_2 solution with different amounts was dropped onto its surface and react for 1.0 min. Finally, the fluorescence signal was collected by a mobile phone (Huawei Mate 20), and corresponding RGB values were obtained through the signal transduction in a Color Picker APP.

For solid detection of glucose, the paper biosensor was fabricated through successively dropping 3 μL of TPE-BTD solution (50 μM) and 3 μL of PB containing 2.0 mM dopamine, 1 mg/mL HRP and 20 $\mu\text{g/mL}$ GOx onto the cellulose paper's surface, and was denoted as TDHG-PS. Then 3 μL of glucose solution with different amounts was dropped onto its surface and react for 20 min. The collection and process of data were carried out according to procedures for solid detection of H_2O_2 .

For solid detection of G-quadruplex DNA and Dam MTase, the paper biosensor was fabricated through successively dropping 3 μL of TPE-BTD solution (50 μM) and 3 μL of 2.0 mM dopamine solution onto the cellulose paper's surface, and was denoted as TD-PS. 3 μL of mixed solution containing 4 μM hemin, 1.0 mM H_2O_2 , and G-quadruplex DNA with different concentrations was dropped onto TD-PS's surface and react for 20 min. The data was recorded for detection of G-quadruplex DNA. The steps for solid detection of Dam MTase were similar to that for Dam MTase assay in solution.

3. Results and discussion

3.1. Characterizations of TPE-BTD

AIEgens with long emission wavelength have attracted considerable attentions from researchers due to the capability of decreasing the interference of background fluorescence. In this context, TPE-BTD with orange emission color was prepared through palladium-catalyzed Heck reaction between TPE-V and BT-D2Br following the preparation route shown in Fig. 1A. The molecular structure of TPE-BTD was confirmed by Fourier transform infrared (FT-IR) and nuclear magnetic resonance (NMR) spectra (Figs. S1 and S2). TPE-BTD emitted strong fluorescence at 550 nm with absolute quantum yield of 0.2311 under 420 nm excitation (Fig. S3). In addition, transient state fluorescence of TPE-BTD revealed a lifetime of 0.9608 ns (Fig. S4). Further, PB-dependent experiment indicated that TPE-BTD solution demonstrated slight fluorescence emission at PB content <30%. At increased PB content, a gradually enhanced FL intensity was recorded, and the intensity arrived at a maximum peak with PB content of 99% (Fig. 1B). Fluorescent images of TPE-BTD at different PB contents, in Fig. 1C, directly validated the phenomenon that TPE-BTD displayed slight emission at PB < 40%, and exhibited gradually enhanced emission when PB content exceed 40%. In addition, it was noted that the maximum emission wavelength displayed obvious blue shift after the PB content of 50%, which might be due to the different packing arrangements of TPE-BTD and was in good line with previously reported works (Dong et al., 2007; Li et al., 2010). From these fluorescent data, there is no doubt that TPE-BTD enjoys exceptional AIE feature.

3.2. Investigation of HRP or H₂O₂-Actuated fluorescence quenching

To authenticate our hypothesis, we integrate TPE-BTD with dopamine to construct a fluorescence assay for HRP or H₂O₂, and the working mechanism was illustrated in Fig. 2A. TPE-BTD and dopamine system displayed bright emission. Whereas, with HRP and H₂O₂ being added, dopamine was catalyzed oxidation into dopachrome by H₂O₂ with the aid of HRP, further initiating the IFE to quench the fluorescence of TPE-BTD due to the overlap of emission spectrum of TPE-BTD and UV-vis spectrum of dopachrome (Fig. S5), displaying unique response to HRP and H₂O₂. The detailed data can be observed in Fig. 2B. TPE-BTD/dopamine system emitted strong fluorescence with intensity of 645 a. u. Contrast experiments implied individual addition of HRP or H₂O₂ did not influence the FL intensity. Upon the simultaneous addition of HRP and H₂O₂, a 66.5-percent intensity decrease was recorded. Moreover, the response is rapid and FL intensity leveled off within only 5 min

(Fig. 2C), which is relatively small compared with that of previously developed H₂O₂ sensors (Gong et al., 2017; Liu et al., 2016; Yuan et al., 2015). Further, we employed TPE-BTD/dopamine system to quantitatively detect H₂O₂. The curves in Fig. 2D and E suggested that FL intensity (F) was in linearly negative proportion to H₂O₂ amounts (C) in the range of 0.01–5.0 μ M, with resulting equation of $F = -80.30 C + 612.26$, coefficient of 0.9847, and detection limit of 4.7 nM. Finally, the expression level of H₂O₂ in MCF-7 cells was determined to evaluate the potential application of TPE-BTD/dopamine system in biological samples. The curves in Fig. S6 demonstrated that when phorbol 12-myristate 13-acetate (PMA) did not exist, slight decrease in FL intensity was recorded in cell lysate. In contrast, after the stimulation of 1.0 μ g/mL PMA, a significantly reduced FL intensity was determined, implying the generation of H₂O₂ under the stimulation of PMA. Based on the decrease in FL intensity, the level of H₂O₂ in PMA-incubated cells was determined to be approximately 3.65 fmol/cell, keeping good line with that of previously reported sensors (Liu et al., 2019; Srikun et al., 2008).

Profiting from the HRP-like activity of hemin/G-quadruplex, TPE-BTD/dopamine system was configured into bioassay for specifically recognizing G-quadruplex DNA. G-quadruplex DNA binds with hemin to form hemin/G-quadruplex, which catalyzed oxidation of dopamine into dopachrome in the presence of H₂O₂, subsequently initiating IFE and quenching fluorescence emission (Fig. 3A). On the basis of the decrease in FL intensity, sensitive detection of G-quadruplex DNA was readily achieved. The data of feasibility experiments was manifested in Fig. 3B. Obviously, addition of hemin and H₂O₂ caused negligible affect on FL intensity, whereas further addition of G-quadruplex DNA T1 resulted in a considerably decreased emission. Again, it only requires 10 min to finish the detection reaction (Fig. 3C). Furthermore, in the range of 0.5–80 nM, FL intensity changed linearly and negatively to T1 with R^2 of 0.9859 and detection limit of 0.21 nM (Fig. 3D and E). Since hemin/G-quadruplex only originated from G-quadruplex DNA, therefore, specific and versatile detection of G-quadruplex DNA can be assured. Fluorescence measurements in Fig. S7 revealed that N1 or N2 or N3 makes little dedication to fluorescence quenching, and T1 or T2 or T3 obviously quenched TPE-BTD's fluorescence, justifying the selectivity and versatility of the TPE-BTD/dopamine sensing system.

3.3. Fluorescence detection of glucose and Dam MTase based on target-induced signal transduction

Benefitting from the multi-component advantages of enzyme-assisted signal transduction reaction, it is inferred that TPE-BTD/dopamine system is applicable for other biomolecules, such as glucose and Dam MTase. To verify this, we first employed TPE-BTD/dopamine

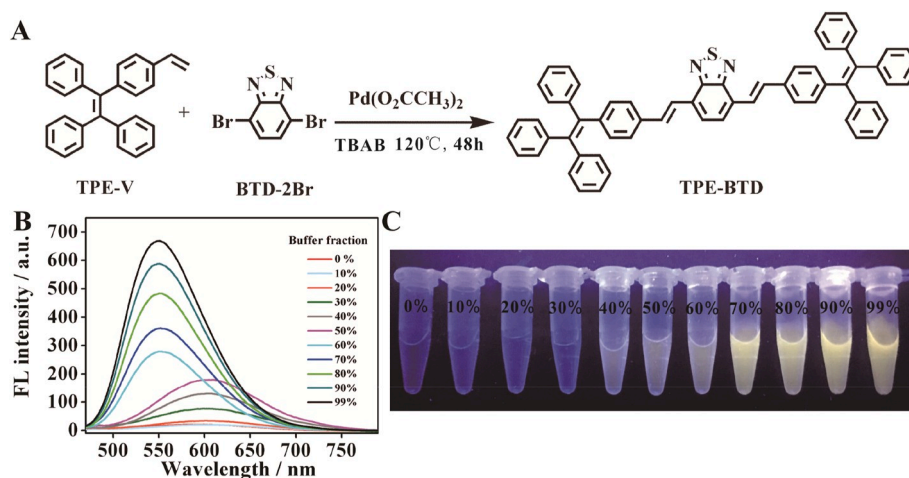


Fig. 1. (A) Synthetic route for TPE-BTD. (B) Fluorescence curves of TPE-BTD in DMSO-PB mixed solution. (C) Images of TPE-BTD in DMSO-PB mixed solution under 365 nm light excitation.

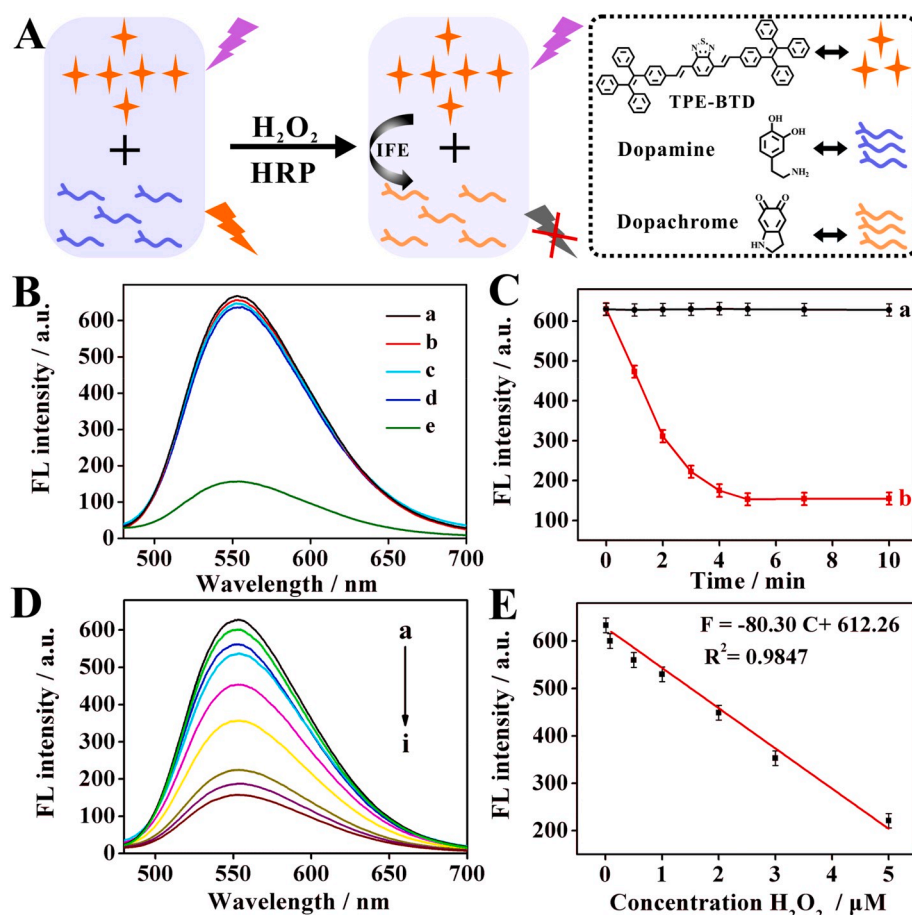


Fig. 2. (A) Scheme illustration of TPE-BTD/dopamine system for H₂O₂/HRP biosensing. (B) Fluorescence spectra of the sensing system: (a) TPE-BTD; (b) TPE-BTD + dopamine; (c) TPE-BTD + dopamine + HRP; (d) TPE-BTD + dopamine + H₂O₂; (e) TPE-BTD + dopamine + HRP + H₂O₂. (C) FL intensity versus incubation time: (a) TPE-BTD + dopamine; (b) TPE-BTD + dopamine + HRP + H₂O₂. (D) Fluorescence spectra of the sensing system corresponding to different H₂O₂ amounts: 0.01, 0.08, 0.5, 1, 2, 3, 5, 10, 50 μM. (E) Linear relationship between FL intensity and H₂O₂ concentration.

system to determine glucose in the presence of GOx and HRP. Glucose was catalyzed by GOx to yield H₂O₂, which was utilized for HRP-induced catalytic oxidation of dopamine into dopachrome, thereby switching IFE and quenching the fluorescence emission (Fig. 4A). Nevertheless, in the absence of glucose, H₂O₂ wasn't formed, and thus dopamine wasn't catalyzed oxidation into dopachrome, resulting in no IFE. As a result, the fluorescence emission was not quenched. Fluorescence characterizations demonstrated that GOx and HRP made little influence on FL intensity (Fig. 4B). Upon the addition of glucose, FL intensity with 71.6-percent decrease was recorded within 20 min (Fig. 4C). A linear equation was obtained between FL intensity and glucose concentration in the range of 0.05–5 μM with R² of 0.9902 (Fig. 4D and E). The detection limit was calculated to be 0.016 μM, which is lower than that of conventional dyes-based glucose biosensors (Table S2). Meanwhile, the proposed system displayed exceptional selectivity for glucose biosensing against lactose, fructose, sucrose, maltose (Fig. S8). Further, we applied TPE-BTD/dopamine system to analyze glucose in serum obtained from a diabetic person, and compared the results with a commercial blood glucose monitor. The serum sample was diluted to make glucose level existing in the range of 0.05–5 μM. The data determined by our method was in good line with that from blood glucose monitor (Table S3), and corresponds well to the expression level of glucose in serum of diabetic person.

To broaden the application range, we further configured TPE-BTD/dopamine system into Dam MTase biosensor based on the enzyme-assisted exponential isothermal amplification reaction (EXPAR). ON1 has the Dam MTase-recognizable sequences, and ON2 was divided by Nb.BbvCI Nease recognition sequences into two parts, one of which has the sequences complementary to s1 derived from the cleavage of ON1 by Dam MTase and the other one has the sequences complementary to G-quadruplex DNA. In the absence of target Dam MTase, the

configurations of ON1 and ON2 didn't change, subsequently leading to no generation of G-quadruplex DNA, and thus the fluorescence of TPE-BTD wasn't quenched. Upon the addition of Dam MTase, s1 was released from ON1 and hybridized with ON2 to initiated EXPAR with the aid of KF polymerase and Nb.BbvCI Nease. Consequently, large amounts of G-quadruplex DNA generated, resulting in a significantly reduced fluorescence (Fig. 5A). The information in Fig. S9A demonstrated that only target Dam MTase could initiate the fluorescence quenching of TPE-BTD. The gradually decreased emission in Fig. S9B indicated that TPE-BTD/dopamine system serves as a biosensor for quantitative detection of Dam MTase. The linear range was determined to be 0.02–20 U/mL, and detection limit was calculated to be 0.0076 U/mL (Fig. S9C), which is comparable to that of previously reported fluorescence biosensors (Table S4). Considering that Dam MTase is highly specific for 5'-GATC-3' in dsDNA, TPE-BTD/dopamine sensing system displayed highly efficient discrimination ability of Dam MTase over other MTases (Fig. S9D). Furthermore, Dam MTase being spiked in serum sample was analyzed by our sensor with acceptable recoveries and low RSDs (Table S5), justifying the sufficiency for practical application in biological fluids.

3.4. Development of AIEgen-Based paper biosensor

Taking into account that AIEgen possessed high emission performance in aggregated state, we thus configured TPE-BTD and dopamine into cellulose paper for solid, equipment-free, and visual detection of target biomarkers. For H₂O₂ assay (Fig. 5B), TDH-PS emitted bright fluorescence, the intensity of which is about the same as that of TPE-BTD on the surface of paper, suggesting the little affect of dopamine and HRP on TPE-BTD's fluorescence in aggregated state. With H₂O₂ being added and concentration increasing, the emission brightness gradually

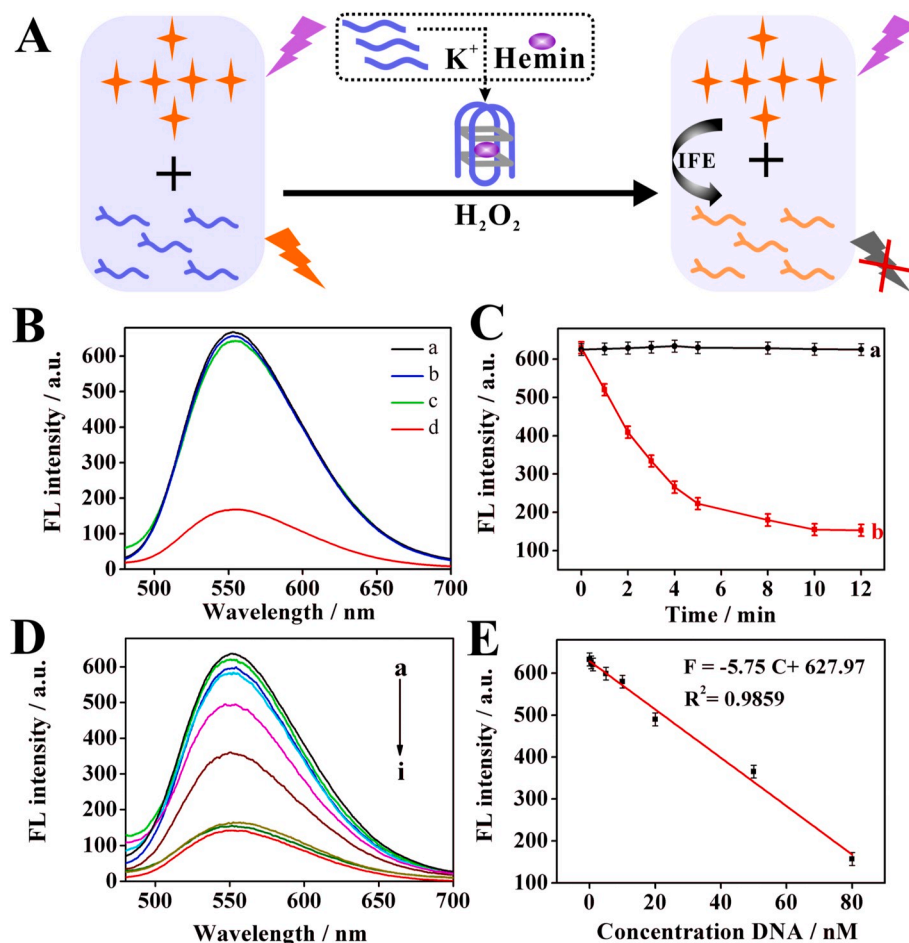


Fig. 3. (A) Scheme illustration of TPE-BTD/dopamine system for G-quadruplex DNA biosensing. (B) Fluorescence spectra of the sensing system: (a) TPE-BTD; (b) TPE-BTD + dopamine; (c) TPE-BTD + dopamine + hemin + H_2O_2 ; (d) TPE-BTD + dopamine + hemin + H_2O_2 + T1. (C) FL intensity versus incubation time: (a) TPE-BTD + dopamine; (b) TPE-BTD + dopamine + hemin + H_2O_2 + T1. (D) Fluorescence spectra of the sensing system corresponding to different T1 amounts: 0.5, 1, 5, 10, 20, 50, 80, 100, 500 nM. (E) Linear relationship between FL intensity and T1 concentration.

diminished (Fig. 5C). From the change in emission brightness recorded by naked eyes, the minimum H_2O_2 level was analyzed to be 0.6 μM . Further, a color picker tool in mobile phone was employed to collect RGB values of TDH-PS to quantitative probe H_2O_2 , and the results were depicted in Fig. 5D. Evidently, R/B value was linearly related to H_2O_2 concentration in the range of 0.6–200 μM with R^2 of 0.9630 and detection limit of 0.23 μM .

Further, TPE-BTD, dopamine, HRP, and GOx were integrated into cellulose paper (TDHG-PS) for glucose assay (Fig. 6). The results demonstrated that when glucose solution drops on TDHG-PS, its emission color gradually fades and eventually turns into colorless with an elevating in glucose amount from 2 to 260 μM . Quantitation analysis showed R/B ratio possesses an excellent linear relationship with R^2 of 0.9671 and a detection limit of 0.84 μM . Meanwhile, we investigated the utilization of TDHG-PS in the analysis of glucose in serum from diabetic person. As displayed in Fig. 6D, a drop of diluted serum on TDHG-PS causes naked-eye color variation, and the color changed along with the increasing glucose amount, justifying the requirement for glucose naked-eye detection in biological samples. According to the sensing principle, excellent response of TD-PS on G-quadruplex DNA and Dam MTase can be also guaranteed, and the detailed information was depicted in Figs. S10 and S11, respectively. These information firmly revealed that our strategy is competent for developing paper biosensor for target biomarkers detection, and that the high fluorescence emission and strong emission stability of TPE-BTD provide significant advantages, as conventional dyes suffered from the serious ACQ effect, going against the solid biosensor invention.

4. Conclusions

In summary, a well-defined TPE-BTD/dopamine system was successfully developed, and when HRP/ H_2O_2 or G-quadruplex/hemin/ H_2O_2 was present, it underwent catalytic oxidation related with fluorescence diminishing due to activated IFE. Thus, TPE-BTD/dopamine system can work as a powerful fluorescence biosensor for H_2O_2 , and G-quadruplex DNA analysis. Coupling with enzyme-assisted signal transduction strategy, we further display that TPE-BTD/dopamine system can be configured into glucose and Dam MTase biosensors, respectively. Moreover, TPE-BTD/dopamine system can be also configured into cellulose paper to fabricate paper biosensors for realizing H_2O_2 , G-quadruplex DNA, glucose, and Dam MTase solid, equipment-free, and visual detection. Overall, this work offered a versatile and label-free strategy for high-performance biosensors development based on AIEgen. We infer this strategy will not only find more use in bio-analytical field, but also broaden AIEgens' application prospect, especially in solid biosensor.

5. Novelty statement

We believe that our result is impressive to the wide and diverse readership of the journal. In this study, we prepared a typical AIE dye (TPE-BTD), and integrated it with dopamine to develop a high-performance biosensor for label-free and sensitive detection of multiple biomarkers in solution state and solid state based on the target-initiated catalyzed oxidation. TPE-BTD, comprising tetraphenylethene and benzothiadiazole moieties, presented strong orange fluorescence emission with absolute quantum yield of 0.2311 and fluorescence

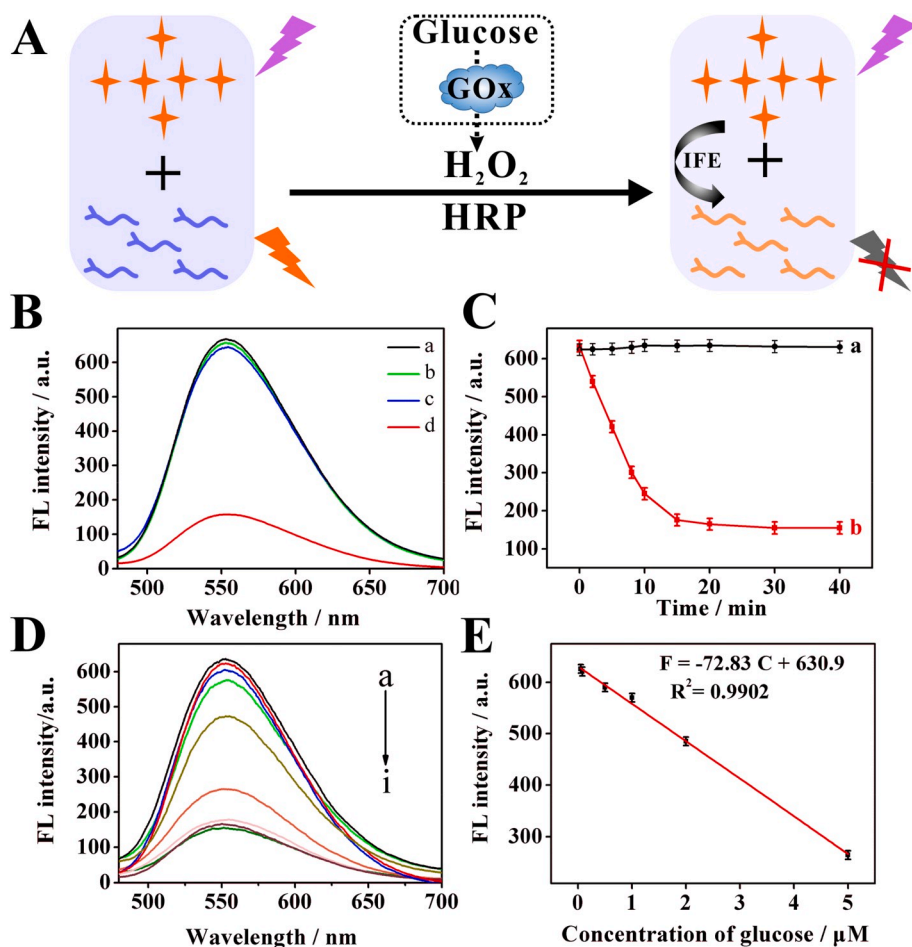


Fig. 4. (A) Scheme illustration of TPE-BTD/dopamine system for glucose biosensing. (B) Fluorescence spectra of the sensing system: (a) TPE-BTD; (b) TPE-BTD + dopamine; (c) TPE-BTD + dopamine + HRP + GOx; (d) TPE-BTD + dopamine + HRP + GOx + glucose. (C) FL intensity versus incubation time: (a) TPE-BTD + dopamine; (b) TPE-BTD + dopamine + HRP + GOx + glucose. (D) Fluorescence spectra of the sensing system corresponding to different glucose amounts: 0.05, 0.08, 0.5, 1, 2, 5, 10, 50, 100 μM . (E) Linear relationship between FL intensity and glucose concentration.

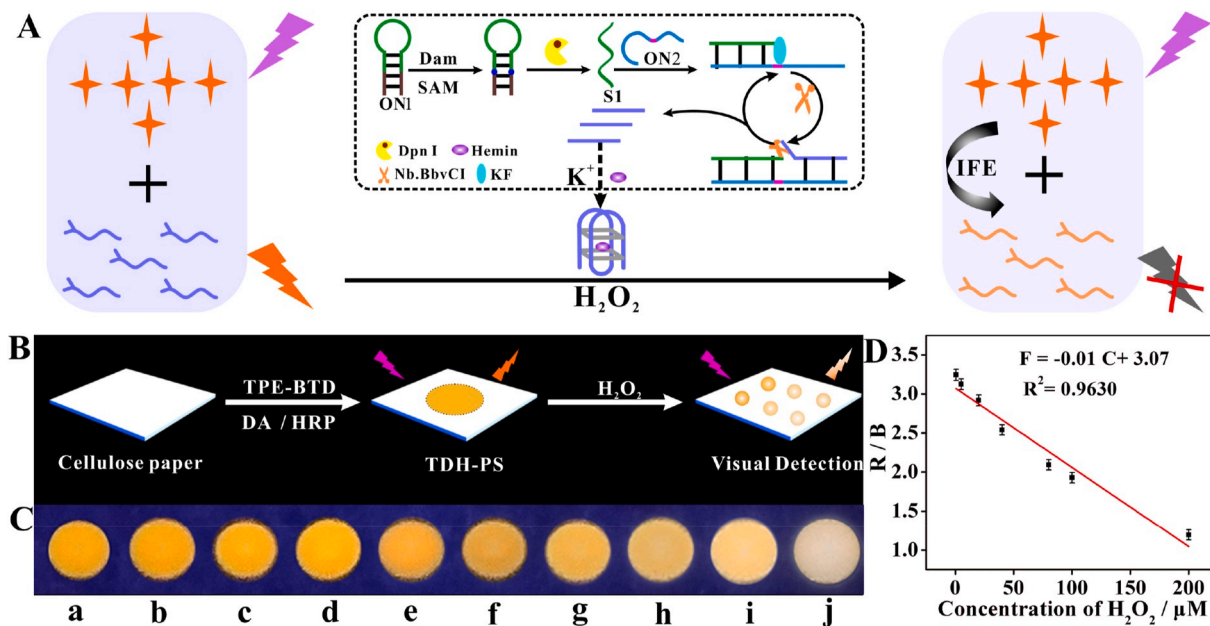


Fig. 5. (A) Scheme illustration of TPE-BTD/dopamine system for sensitive detection of Dam MTase based on the target-initiated EXPAR. (B) Scheme illustration for TDH-PS fabrication and its application in detection of H_2O_2 . (C) Fluorescent images of different samples: (a) TPE-BTD; (b) TPE-BTD + dopamine; (c) TDH-PS; from (d) to (j) H_2O_2 concentration was 0.6, 5, 20, 40, 80, 100, 200 μM , respectively. (D) Linear relationship between R/B value and H_2O_2 concentration.

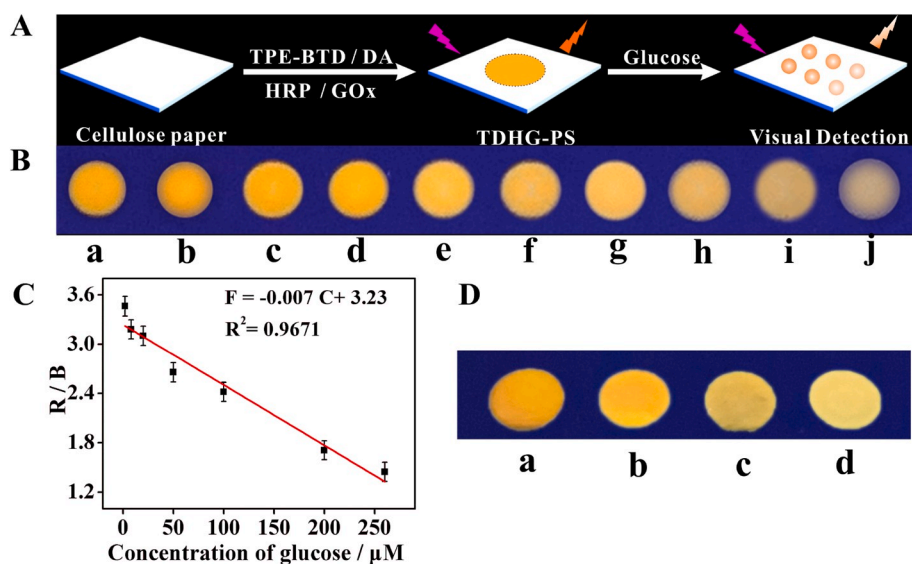


Fig. 6. (A) Scheme illustration for TDHG-PS fabrication and its application in detection of glucose. (B) Fluorescent images of different samples: (a) TPE-BTD; (b) TPE-BTD + dopamine; (c) TDHG-PS; from (d) to (j) glucose concentration was 2, 8, 20, 50, 100, 200, 260 μM respectively. (C) Linear relationship between R/B value and H_2O_2 concentration. (D) Real sample analysis of TDHG-PS: (a) TDHG-PS, (b) TDHG-PS + diluted serum, (c) TDHG-PS + diluted serum + 100 μM glucose, (d) TDHG-PS + diluted serum + 200 μM glucose.

lifetime of 0.9608 ns. However, its emission can be quenched by dopachrome originating from the catalyzing oxidation of HRP and H_2O_2 on dopamine based on inner filter effect (IFE) due to the overlap of emission spectrum of TPE-BTD and UV-vis curve of dopachrome, demonstrating highly sensitive response to H_2O_2 . Since hemin/G-quadruplex possesses high HRP-like activity, G-quadruplex DNA and H_2O_2 can generate through target-switched transduction reaction, TPE-BTD/dopamine system was applicable for G-quadruplex DNA and other biomarkers biosensing. Finally, TPE-BTD was employed as emitters in fabrication of paper biosensors, which can achieve solid, equipment-free and visual detection of multiple biomarkers based on the high emission performance of TPE-BTD, opening up a new pathway to development of biosensors for practical application. We expect this sensing conception will be helpful in development of practical biosensors, and this sensor will find more applications in disease diagnosis.

Declaration of competing interest

The authors declare that they have no known competing financial interests or personal relationships that could have appeared to influence the work reported in this paper.

CRediT authorship contribution statement

Haiyin Li: Conceptualization, Data curation, Investigation, Methodology, Formal analysis, Software. **Haiyang Lin:** Conceptualization, Investigation, Methodology, Data curation, Software. **Wenxin Lv:** Conceptualization, Data curation, Investigation, Methodology. **Panpan Gai:** Project administration, Software, Supervision, Resources. **Feng Li:** Funding acquisition, Project administration, Resources.

Acknowledgements

This work was funded by the National Natural Science Foundation of China (21605093 and 21775082), the Shandong Province Higher Educational Program for Young Innovation Talents, the Major Program of Shandong Province Natural Science Foundation (ZR2018ZC0127), and the Special Foundation for Distinguished Taishan Scholar of Shandong Province (ts201511052).

Appendix A. Supplementary data

Supplementary data to this article can be found online at <https://doi.org/10.1016/j.bios.2020.112336>.

[org/10.1016/j.bios.2020.112336](https://doi.org/10.1016/j.bios.2020.112336).

References

- Adhikary, R., Mukherjee, P., Krishnamoorthy, G., Kunkle, R.A., Casey, T.A., Rasmussen, M.A., Petrich, J.W., 2010. Anal. Chem. 82 (10), 4097–4010.
- Albada, H.B., Golub, E., Willner, I., 2016. Chem. Sci. 7 (5), 3092–3101.
- Broza, Y.Y., Zhou, X., Yuan, M., Qu, D., Zheng, Y., Vishinkin, R., Khatib, M., Wu, W., Haick, H., 2019. Chem. Rev. 119 (22), 11761–11817.
- Chang, J.F., Wang, X., Wang, J., Li, H.Y., Li, F., 2019. Anal. Chem. 91 (5), 3604–3610.
- Chinen, A.B., Guan, C.M., Ferrer, J.R., Barnaby, S.N., Merkel, T.J., Mirkin, C.A., 2015. Chem. Rev. 115 (19), 10530–10574.
- Das, P.M., Singal, R., 2004. J. Clin. Oncol. 22 (22), 4632–4642.
- Ding, D., Li, K., Liu, B., Tang, B.Z., 2013. Acc. Chem. Res. 46 (11), 2441–2453.
- Dong, Y.Q., Lam, J.W.Y., Qin, A.J., Sun, J.X., Liu, J.Z., Li, Z., Sun, J.Z., Sung, H.H.Y., Williams, I.D., Kwok, H.S., Tang, B.Z., 2007. Chem. Commun. 31, 3255–3257.
- Feng, H., Zhang, Z.Q., Meng, Q.T., Jia, H.M., Wang, Y., Zhang, R., 2018a. Adv. Sci. 5 (8), 1800397, 1800391–1800310.
- Feng, H.T., Yuan, Y.X., Xiong, J.B., Zheng, Y.S., Tang, B.Z., 2018b. Chem. Soc. Rev. 47 (19), 7452–7476.
- Ghosh, S., Ghosal, K., Mohammad, S.A., Sarkar, K., 2019. Chem. Eng. J. 373, 468–484.
- Golub, E., Freeman, R., Willner, I., 2011. Angew. Chem. Int. Ed. 50 (49), 11710–11714.
- Gong, T.T., Liu, J.F., Wu, Y.W., Xiao, Y., Wang, X.H., Yuan, S.Q., 2017. Biosens. Bioelectron. 92, 16–20.
- Hu, J., Wang, S.Q., Wang, L., Li, F., Pingguan-Murphy, B., Lu, T.J., Xu, F., 2014. Biosens. Bioelectron. 54, 585–597.
- Huang, Y.F., Zhang, M., Zhao, L.B., Feng, J.M., Wu, D.Y., Ren, B., Tian, Z.Q., 2014. Angew. Chem. Int. Ed. 53 (9), 2353–2357.
- Jia, R.N., Tian, W.G., Bai, H.T., Zhang, J.M., Wang, S., Zhang, J., 2019. Nat. Commun. 10 (1), 791–798, 795.
- Lemon, C.M., Karnas, E., Han, X.X., Bruns, O.T., Kempa, T.J., Fukumura, D., Bawendi, M. G., Jain, R.K., Duda, D.G., Nocera, D.G., 2015. J. Am. Chem. Soc. 137 (31), 9832–9842.
- Li, H.Y., Chi, Z.G., Xu, B.J., Zhang, X.Q., Yang, Z.Y., Li, X.F., Liu, S.W., Zhang, Y., Xu, J. R., 2010. J. Mater. Chem. 20 (29), 6103–6110.
- Li, H.Y., Chang, J.F., Gai, P.P., Li, F., 2018. ACS Appl. Mater. Interfaces 10 (5), 4561–4568.
- Li, Z., Askim, J.R., Suslick, K.S., 2019. Chem. Rev. 119 (1), 231–292.
- Liu, R., Wang, X.D., Aihara, K., Chen, L.N., 2014. Med. Res. Rev. 34 (3), 455–478.
- Liu, J.W., Luo, Y., Wang, Y.M., Duan, L.Y., Jiang, J.H., Yu, R.Q., 2016. ACS Appl. Mater. Interfaces 8 (49), 33439–33445.
- Liu, F.J., Yang, L.M., Yin, X.H., Liu, X.J., Ge, L., Li, F., 2019. Biosens. Bioelectron. 141, 111446.
- Miao, X.M., Cheng, Z.Y., Ma, H.Y., Li, Z.B., Xue, N., Wang, P., 2018. Anal. Chem. 90 (2), 1098–1103.
- Min, X.H., Zhuang, Y., Zhang, Z.Y., Jia, Y.M., Hakeem, A., Zheng, F.X., Cheng, Y., Tang, B.Z., Lou, X., Xia, F., 2015. ACS Appl. Mater. Interfaces 7 (30), 16813–16818.
- Muthusankar, G., Devi, R.K., Gopu, G., 2020. Biosens. Bioelectron. 150, 111947.
- Niu, S.Y., Bi, C., Song, W.L., 2020. Anal. Biochem. 590, 113532.
- Parolo, C., Merkoci, A., 2013. Chem. Soc. Rev. 42 (2), 450–457.
- Shahrokhian, S., Khaki Sanati, E., Hosseini, H., 2018. Biosens. Bioelectron. 112, 100–107.
- Shi, J., Deng, Q., Wan, C., Zheng, M., Huang, F., Tang, B., 2017. Chem. Sci. 8 (9), 6188–6195.
- Srikun, D., Miller, E.W., Domaille, D.W., Chang, C.J., 2008. J. Am. Chem. Soc. 130 (14), 4596–4597.

- Tagit, O., Hildebrandt, N., 2017. ACS Sens. 2 (1), 31–45.
- Wang, X.R., Hu, J.M., Zhang, G.Y., Liu, S.Y., 2014. J. Am. Chem. Soc. 136 (28), 9890–9893.
- Wang, F.Y., Zhu, Y., Zhou, L., Pan, L., Cui, Z.F., Fei, Q., Luo, S.H., Pan, D., Huang, Q., Wang, R., Zhao, C.C., Tian, H., Fan, C.H., 2015. Angew. Chem. Int. Ed. 54 (25), 7349–7353.
- Wu, L., Qu, X.G., 2015. Chem. Soc. Rev. 44 (10), 2963–2997.
- Yang, Z.Z., Wen, Z.B., Peng, X., Chai, Y.Q., Liang, W.B., Yuan, R., 2019. Chem. Commun. 55 (45), 6453–6456.
- Yuan, J., Cen, Y., Kong, X.J., Wu, S., Liu, C.L., Yu, R.Q., Chu, X., 2015. ACS Appl. Mater. Interfaces 7 (19), 10548–10555.
- Zang, F., Su, Z., Zhou, L., Konduru, K., Kaplan, G., Chou, S.Y., 2019. Adv. Mater. 31 (30), 1902331.
- Zhang, W.H., Ma, W., Long, Y.T., 2016. Anal. Chem. 88 (10), 5131–5136.
- Zhang, K., Song, S., Yang, L., Min, Q., Wu, X., Zhu, J.J., 2018. Chem. Commun. 54 (93), 13131–13134.
- Zhang, J.J., Chai, X.Z., He, X.P., Kim, H.J., Yoon, J., Tian, H., 2019. Chem. Soc. Rev. 48 (2), 683–722.
- Zhu, L.Y., Li, Y., Zhang, L., Wen, Y.J., Ju, H.X., Lei, J.P., 2020. Anal. Chim. Acta 1094, 130–135.